Valley Acoustoelectric Effect

A. V. Kalameitsev,[1] V. M. Kovalev,[1,2] and I. G. Savenko[3,1,*]
[1]*Rzhanov Institute of Semiconductor Physics SB RAS, 630090 Novosibirsk, Russia*
[2]*Novosibirsk State Technical University, Novosibirsk, 630072 Russia*
[3]*Center for Theoretical Physics of Complex Systems, Institute for Basic Science (IBS), Daejeon 34126, Korea*

(Received 1 March 2019; published 26 June 2019)

We report on the novel valley acoustoelectric effect, which can arise in a 2D material, like a transition metal dichalcogenide monolayer, residing on a piezoelectric substrate. The essence of this effect lies in the emergence of a drag electric current (and a spin current) due to a propagating surface acoustic wave. This current consists of three contributions, one independent of the valley index and proportional to the acoustic wave vector, the other arising due to the trigonal warping of the electron dispersion, and the third one is due to the Berry phase, which Bloch electrons acquire traveling along the crystal. As a result, there appear components of the current orthogonal to the acoustic wave vector. Further, we build an angular pattern, encompassing nontrivial topological properties of the acoustoelectric current, and suggest a way to run and measure the conventional diffusive, warping, and acoustoelectric valley Hall currents independently. We develop a theory, which opens a way to manipulate valley transport by acoustic methods, expanding the applicability of valleytronic effects on acoustoelectronic devices.

DOI: 10.1103/PhysRevLett.122.256801

Two-dimensional materials (2D materials), such as transition metal dichalcogenides (TMD) [1–3], possess symmetry properties similar to graphene [4]. Their primary feature is that the valleys K and K' in the Brillouin zone connect by time-reversal symmetry. Consequently, the chiralities of the K and K' bands turn out opposite, and in addition to conventional momentum and spin of the two-dimensional electron gas (2DEG), 2D materials acquire an additional valley index degree of freedom. Moreover, their spectra manifest large gaps in the optical range [5], epitomizing various valley-resolved phenomena [6,7].

Exposed to external strong electromagnetic fields resulting in a dynamical gap opening [8–11], 2D materials can exhibit such fascinating phenomena as dissipationless transport of 2DEG [12] and the photon drag effect [13–16]. Moreover, stemming from the essential spatial inversion symmetry breaking, there might occur transport phenomena described by a third-order conductivity tensor [14,17], finite in noncentrosymmetric materials. For example, in the photovoltaic effect [18], the conductivity tensor χ couples components of the photoinduced current j_α with the components of the external electric field E_β: $j_\alpha = \chi_{\alpha\beta\gamma} E_\beta E_\gamma$, where $\alpha, \beta, \gamma = x, y, z$.

The conventional photovoltaic effect originates from an asymmetry of the interaction potential or the Bloch wave function [19]. In 2D materials, there can also appear an unconventional mechanism of this effect, which is due to the trigonal warping of the valley spectrum, resulting in the asymmetry of the interband optical transitions [20]. In addition to the valley and spin currents [21–23], trigonal warping also manifests itself in the second-harmonic generation phenomena [24], spin-resolved measurements of the photoluminescence from the sample, and alignment of the photoexcited carriers in gapless materials [25].

Only a few phenomena distinguish Bloch electrons from free charges, and one of them is the Berry effect, which, in particular, influences the carriers of charge subject to a mechanical force $e\mathbf{E}$, where $\mathbf{E}$ is an external electric field and e is the elementary charge. It happens since the group velocity of a Bloch electron acquires an additional anomalous term $e\mathbf{E} \times \mathbf{\Omega}_\mathbf{k}$, where $\mathbf{k}$ is the momentum of the particle and $\mathbf{\Omega}_\mathbf{k}$ is the Berry curvature [2,26]. In the framework of the linear response theory, the matrix of the velocity operator acquires nonzero off-diagonal linear in field elements, thus mixing different bands.

The concept of the Berry phase [27] underlies and unifies diverse aspects of solid-state physics, drastically affecting the transport of particles and resulting in such intriguing phenomena as the anomalous [28] and quantum [29] Hall effects, emergence of topological and superconducting phases [30], charge pumping [31], and anomalous thermoelectric transport [32], among other [33]. By and large, electrons in a crystal behave similarly to free particles with just the free-electron mass replaced by an effective one due to the formation of energy bands. A nontrivial Berry phase also reveals itself in Dirac materials like graphene [34], and very recently it has come into play in other two-dimensional materials [35], possessing similar symmetry properties.

Instead of light, surface acoustic waves (SAWs) can be employed to probe or alter the physical properties of electron (and other) gases in low-dimensional systems

[36,37]. It is relatively simple to launch SAWs in piezoelectric heterostructures. That is why SAWs are frequently used in engineering and scientific applications, forming the basis of acoustoelectronics. The appearance of new 2D materials stimulates the studies of SAWs, interacting with electrons in graphene monolayers [38,39], surfaces of topological insulators [40], and thin films [41]. Recently, there have been suggested SAW spectroscopy methods to study 2D dipolar exciton gases in normal and Bose-condensed phases [42,43], including the acoustic drag effect [44]. Experimentally, one can either (i) measure the absorption of sound by a 2DEG, (ii) observe renormalization of the SAW velocity in heterostructures exposed to strong magnetic fields [45] due to their interaction with the carriers of charge, or (iii) study the acoustoelectric (AE) effect. The latter consists in the emergence of stationary electric currents when a SAW drags the carriers of charge via the momentum transfer to the 2DEG [46].

In this Letter, we demonstrate that in multivalley 2D materials, there takes place an unconventional AE effect and an AE valley Hall effect (AVHE). We consider a TMD monolayer, taking MoS_2 as an example, and show that the trigonal valley warping gives an additional component of the AE current with peculiar properties, characteristic of 2D materials (we will call this component the warping current). Furthermore, the Berry effect gives an unconventional acoustic drag Hall current. It is known [33] that if a TMD monolayer is exposed to an in-plane static electric field, the Berry curvature allows for the appearance of the valley Hall effect, when the current flows in the direction transverse to the static in-plane electric field. If we take an ac instead of the static field, the stationary valley Hall current is absent since the time-averaged force acting on electrons vanishes. However, a nonzero force appears in the second order with respect to the ac electric field. Here we consider the case when such a force is due to the piezoelectric field of the surface acoustic waves, traveling along the surface of the piezoelectric substrate. We show that the joint influence of this force and the Berry phase allow for the AVHE. These currents couple with the piezoelectric field of an external acoustic wave via the third-order conductivity tensor, as in the photovoltaic effect mentioned above, forming various fascinating propagation patterns. Moreover, the SAWs aspire to separate particles with opposite spins, resulting in a spin current.

Let us consider a layer of MoS_2, separated from a piezoelectric substrate by a dielectric layer (Fig. 1). A Bleustein-Gulyaev SAW with the wave vector $\mathbf{k}$ travels along the interface and creates a piezoelectric field having both the out-of-plane and in-plane components. The latter is $\mathbf{E}||\mathbf{k}$ and it acts on the 2DEG. This field drags the carriers of charge in MoS_2, resulting in the AE current. We assume that the monolayer is n doped. Furthermore, the conduction band in each of the valleys is split by spin due to the spin-orbit interaction (SOI), as is shown in Fig. 2(a); the strength of the SOI for MoS_2 is of the order of 3 meV [47].

The group velocity describing the quasiclassical dynamics of a Bloch electron in the absence of an external magnetic field reads

$$\dot{\mathbf{r}} = \mathbf{v} - \dot{\mathbf{p}} \times \mathbf{\Omega}_{\mathbf{p}}, \tag{1}$$

where $\mathbf{v} = \partial\varepsilon_{\mathbf{p}}/\partial\mathbf{p}$, $\varepsilon_{\mathbf{p}} = \mathbf{p}^2/2m + w_{\mathbf{p}}$ is the electron dispersion in a given valley including its warping $w_{\mathbf{p}} = \eta C(p_x^3 - 3p_x p_y^2)$, $\eta = \pm 1$ is a valley index, C is a warping strength, and $\dot{\mathbf{p}} = e\tilde{\mathbf{E}}$ with $e < 0$ the electron charge, and $\tilde{\mathbf{E}}(\mathbf{r}, t) = \tilde{\mathbf{E}} e^{i\mathbf{kr} - i\omega t}/2 + \text{c.c.}$ is the overall electric field, including the piezoelectric $\mathbf{E}(\mathbf{r}, t)$ and induced $\mathbf{E}^i(\mathbf{r}, t)$ contributions. The origin of the induced electric field $\mathbf{E}^i(\mathbf{r}, t)$ is the fluctuations of the electron density. The Berry curvature reads $\mathbf{\Omega}_{\mathbf{p}} = \partial_{\mathbf{p}} \times \langle u | i\partial_{\mathbf{p}} | u \rangle$, and $|u\rangle$ is a periodic amplitude of the Bloch wave function.

To describe the electron transport, we will use the Boltzmann transport equation [48],

$$\frac{\partial f}{\partial t} + \dot{\mathbf{p}} \cdot \frac{\partial f}{\partial \mathbf{p}} + \dot{\mathbf{r}} \cdot \frac{\partial f}{\partial \mathbf{r}} = I\{f\}, \tag{2}$$

where f is the electron distribution function and $I\{f\}$ is the collision integral. For the collision integral we use the model of a single-τ approximation [49], which does not depend on energy: $I\{f\} = -(f - \langle f \rangle)/\tau$. Here $\langle f \rangle$ is the locally equilibrium distribution function in the reference frame moving with the SAW. It depends on the local electron density $N(\mathbf{r}, t)$ via the chemical potential

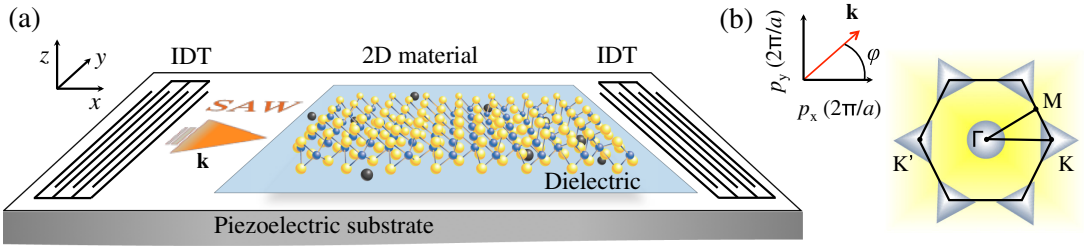

FIG. 1. System schematic. (a) 2D material (MoS_2) exposed to a surface acoustic wave (SAW) with the wave vector $\mathbf{k}$. The sample lies on a layer of dielectric on a piezoelectric substrate. Two interdigital transducers (IDTs) generate and detect the SAWs. (b) The first Brillouin zone of MoS_2 with the schematic illustration of warping.

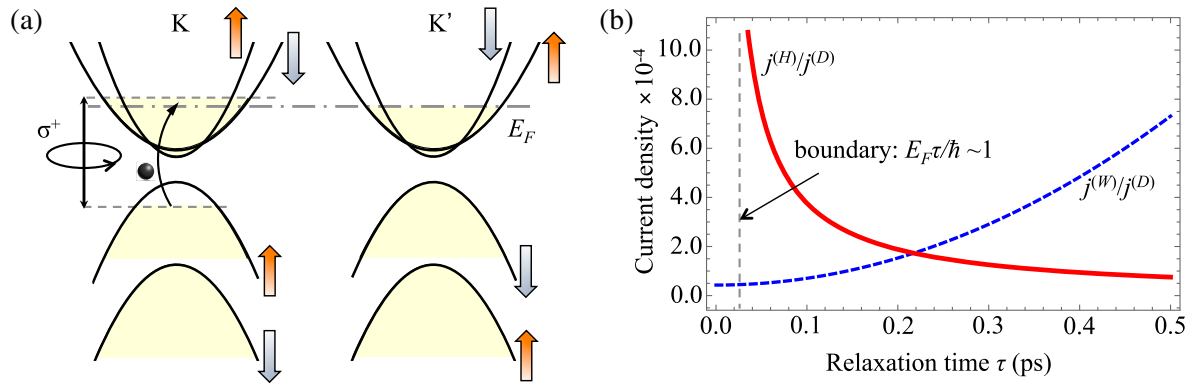

FIG. 2. (a) The band structures of MoS_2 under the optically induced imbalance of the valley populations. Yellow shaded regions indicate the filled states. The arrows signify the directions of spin in each valley. (b) Relative magnitudes of the AE warping (dashed blue curve) and valley Hall (solid red curve) components of the current density as functions of the relaxation time at $n = 5 \times 10^{12}$ cm^{-2}.

$\mu = \mu(N)$. Furthermore, we expand the density in series: $N(\mathbf{r}, t) = n + n_1(\mathbf{r}, t) + n_2(\mathbf{r}, t) + O(n_3)$, where n is the unperturbed electron density and n_i are the corrections to the density fluctuations. We expect that the AE current should appear as the second-order response to the external piezoelectric field. Thus we expand the distribution function: $f = f_0 + f_1 + f_2 + O(f_3)$, where $f_0 = (\exp\{[\varepsilon_{\mathbf{p}} - \mu(n)]/T\} + 1)^{-1}$ is the equilibrium electron distribution, which depends on the electron momentum $\mathbf{p}$ only. We also expand $\langle f \rangle$: $\langle f \rangle = f_0 + (n_1 + n_2 + \cdots)\partial_n f_0 + (n_1 + n_2 + \cdots)^2 \partial^2 f_0/\partial n^2/2$. The induced electric field obeys the Maxwell equation, $\mathrm{div}\mathbf{D}^i = 4\pi\rho$, where $\mathbf{D}^i = \epsilon(z)\mathbf{E}^i$, $\epsilon(z)$ is the dielectric function, and the charge density reads $\rho = e[N(\mathbf{r}, t) - n]\delta(z)$. The solution is $\mathbf{E}^i = -4\pi i e\mathbf{k}(N - n)_{\mathbf{k},\omega}/[(\epsilon + 1)k]$, where ϵ is the dielectric constant of the substrate.

Results and discussion.—Let us, first, assume that the warping and the Berry phase are absent. In this case the drag of electrons is valley independent. For a SAW traveling with the momentum $\mathbf{k}$ and in the long-wavelength limit ($\omega\tau, \mathbf{k}\cdot\mathbf{v}\tau \ll 1$), the drift current is negligibly small, whereas for a degenerate electron gas at zero temperature (which, in particular, gives $\partial\mu/\partial n = \pi/m$), we find the diffusive current (see Supplemental Material [50]),

$$\mathbf{j}^{(D)} = \frac{e\tau}{2m}\frac{\mathbf{k}\sigma}{\omega}\frac{|E_0|^2}{1 + (kv^*/\omega + Dk^2/\omega)^2}, \tag{3}$$

where $\sigma = e^2 n\tau/m$ is a 2D static Drude conductivity with the dimensionality of velocity, $D = v_F^2\tau/2$ is a diffusion coefficient, v_F is the Fermi velocity, $v_* = 4\pi\sigma/(\epsilon + 1)$ is the velocity of charge spreading in 2D systems, and E_0 is the piezoelectric field amplitude. We want to note that Eq. (3) at $Dk^2/kv_* \ll 1$ coincides with the formula of the AE current, reported in Ref. [51].

Now we switch the trigonal warping and the Berry phase on. After derivations [50] we find the components of the current density. Let us compare the AE diffusive, warping [22], and Hall currents. They can be written in the uniform way:

$$\mathbf{j}^{(D)} = \frac{e\sigma k}{2\omega}\frac{\tau}{m}\frac{\mathbf{n}}{1 + (\sigma/\sigma_*)^2(1 + ka)^2}E_0^2, \tag{4}$$

$$\mathbf{j}^{(W)} = e\sigma m\tau\frac{\nabla_{\mathbf{n}} C(\mathbf{n})[1 + (\sigma/\sigma_*)^2(ka)^2]}{1 + (\sigma/\sigma_*)^2(1 + ka)^2}E_0^2, \tag{5}$$

$$\mathbf{j}^{(H)} = \frac{e\sigma k}{2\omega}\frac{[\mathbf{n}\times\boldsymbol{\Omega}_0]}{1 + (\sigma/\sigma_*)^2(1 + ka)^2}E_0^2, \tag{6}$$

where we choose the coordinate axes as in Fig. 1, then $\mathbf{n} = \mathbf{k}/k$, $C(\mathbf{n}) = \eta C(n_x^3 - 3n_x n_y^2)$, $\sigma_* = (\epsilon + 1)s/4\pi$, and $a = (\epsilon + 1)\hbar^2/(4me^2)$. The Berry curvature has an out-of-plane component $\boldsymbol{\Omega}_0 = (0, 0, \hbar\eta/m\Delta)$, where Δ is the band gap of the TMD monolayer. Because of the usual smallness of the warping, we will disregard its contribution to the static conductivity and the charge spreading, when describing the screening effect.

From Eqs. (5) and (6) we see that the net valley AE currents summed over the valley indices $\eta = \pm 1$ are zero, due to the time-reversal symmetry. Hence, it should be broken to detect the valley currents. One of the possible ways to do it is to expose the sample to a circularly polarized light with the frequency close to the band gap since the optical selection rules in 2D materials depend on η; see Fig. 2(a). Then one of the valleys will be dominantly populated. The difference in the particle densities, $\delta n = n(\eta = 1) - n(\eta = -1) \neq 0$, results in a nonzero net valley current.

Let us now estimate relative magnitudes of different contributions to the AE current. For realistic parameters $\sigma/\sigma_* \gg 1$ and $ka \ll 1$, we find

$$j^{(D)} \approx \frac{(\sigma_* E_0)^2}{ens} \approx 20\ \mu\text{A/cm}, \tag{7}$$

where we used the sound velocity $s = 3.5 \times 10^5$ cm/s for the $LiNbO_3$ piezoelectric substrate, acoustic wave piezoelectric potential amplitude $\varphi_{\text{SAW}} = 50$ mV (thus, $E_0 = k\varphi_{\text{SAW}}$), and other parameters read $n = 5 \times 10^{12}$ cm^{-2}, $\tau = 2 \times 10^{-13}$ s, $\omega = 10^{10}$ s^{-1}.

The AVHE contribution stemming from the Berry phase effect relates to the diffusive current as

$$j^{(H)}/j^{(D)} = \frac{\delta n}{n}\frac{\hbar}{\tau\Delta}, \tag{8}$$

whereas for the warping current,

$$j^{(W)}/j^{(D)} = \frac{\delta n}{n}\left(\frac{C_e m s^2}{\hbar^3}\right)[1 + (\sigma/\sigma_*)^2 (ka)^2]. \tag{9}$$

Now taking $C_e = -3.49$ eV Å^3 and $m = 0.44 m_0$ (for MoS_2), $\delta n/n = 0.1$, we find the estimations $j^{(H)} \sim 4$ nA/cm and $j^{(W)} \sim 3$ nA/cm.

Note that the warping and Hall currents depend differently on the relaxation time [see Fig. 2(b)]. The τ dependence of the warping current Eq. (9) is determined by the σ^2 term, whereas the Hall current Eq. (8) grows with the decrease of τ. However, the system imposes the lower boundary of τ dictated by the condition $E_F\tau/\hbar \gg 1$, which implies $\tau \approx 0.2$ ps at $n = 5 \times 10^{12}$ cm^{-2}. The upper boundary is determined by the applicability of the diffusive limit.

The AE Hall and warping currents might have comparable magnitudes in some parameter range, but they possess different topological properties. Indeed, the current densities Eqs. (4)–(6) have the forms $\mathbf{j}^{(D)} = j_0^{(D)}(\cos\varphi, \sin\varphi)$, $\mathbf{j}^{(W)} = j_0^{(W)}(\cos 2\varphi, -\sin 2\varphi)$, and $\mathbf{j}^{(H)} = j_0^{(H)}(\sin\varphi, -\cos\varphi)$, respectively (see Fig. 3). The magnitudes of both the diffusive and Hall current densities are proportional to the SAW wave vector. Thus they behave like the cosine or sine of the angle, describing the direction of propagation of the SAW. In the meantime, the warping-related current originates from the warping of the electron dispersion in the valleys, which behaves as $\cos 3\varphi$ due to the C_{3h} symmetry group. Furthermore, the electron velocity, being the derivative of the energy with respect to the electron momentum, gives the $\cos 2\varphi$ and $\sin 2\varphi$ behavior of the warping-related current density.

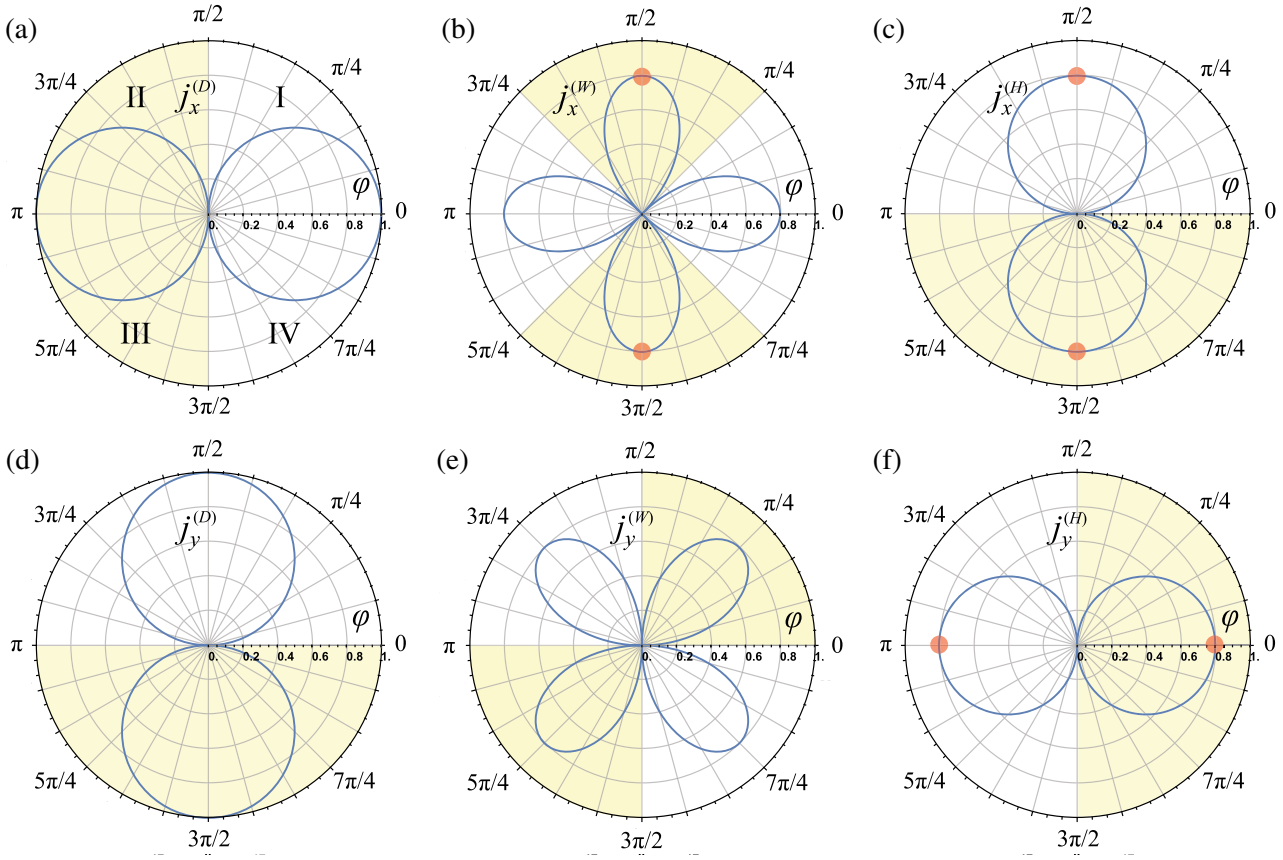

FIG. 3. Angular patterns of the x and y components of the diffusive (a),(d), warping (b),(e), and Hall (c),(f) current density in arbitrary units. The warping and Hall current petals are depicted smaller than the conventional diffusive current petal to show that their magnitudes are smaller. Yellow shading marks the areas of negative current (directed opposite to the x or y axis). Red dots indicate the angles ($\pi/2$, $3\pi/2$, 0, and π), at which only the unconventional current flows along the x or y direction.

Let us consider an acoustic wave propagating along the y direction, which corresponds to $\varphi = \pi/2$ or $\varphi = 3\pi/2$. Then the x component of the diffusive current vanishes, while the x components of the AE Hall and warping currents are nonzero [see Figs. 3(b) and 3(c)]. If $\varphi = \pi/2$, the two currents have opposite direction and partially compensate each other, whereas if $\varphi = 3\pi/2$, the currents sum up. Obviously, it allows us to distinguish between their contributions. If the acoustic wave propagates along the x direction, then $\phi = 0$ or $\phi = \pi$ and only the y component of the Hall current is nonzero [see Fig. 3(f)], while the y components of the diffusive and warping currents vanish.

We want to note that the SOI for the conduction band, being small in comparison with typical optical frequencies, is usually disregarded in optically induced transport effects. We have estimated the relative contributions of the AE warping and Hall currents and shown that they can have comparable magnitudes for the electron densities of the order $n = 5 \times 10^{12}$ cm^{-2}. For such density, the Fermi energy lies deep in the conduction band, exceeding the SO splitting energy (for the MoS_2 it amounts to 3 meV). In these conditions the spin current is negligibly small. A possible way to observe the AE spin effect is to have a p-doped layer with Fermi energy lying in the valence band between the SO-split hole subbands with the splitting ~400 meV for TMD monolayers, which exceeds by orders the SAW frequencies. Obviously, the theory developed in this work is directly applicable to the p-doped TMDs. It should be underlined that spin AE currents might occur even in the case of equal populations of the valleys (in the absence of an external illumination). The emergence of the spin current, together with the electric currents [Eqs. (5) and (6)], are the quintessence of the valley AE effect.

Conclusions.—We have reported on the valley acoustoelectric effect and the valley acoustoelectric Hall effect in noncentrosymmetric materials exposed to surface acoustic waves. We calculated the electric current densities and compared their magnitudes and directions of propagation with the conventional diffusive current, suggesting a way to design topologically diverse patterns of electric current and the spin current.

We have been supported by the Institute for Basic Science in Korea (Project No. IBS-R024-D1) and the Russian Foundation for Basic Research (Project No. 19-42-540011).

*Corresponding author.
ivan.g.savenko@gmail.com

[1] B. Radisavljevic, A. Radenovic, J. Brivio, V. Giacometti, and A. Kis, Single-layer MoS_2 transistors, Nat. Nanotechnol. **6**, 147 (2011).

[2] R. S. Sundaram, M. Engel, A. Lombardo, R. Krupke, A. C. Ferrari, Ph. Avouris, and M. Steiner, Electroluminescence in single layer MoS_2, Nano Lett. **13**, 1416 (2013).

[3] X. Xu, W. Yao, D. Xiao, and T. F. Heinz, Spin and pseudospins in layered transition metal dichalcogenides, Nat. Phys. **10**, 343 (2014).

[4] K. S. Novoselov, A. K. Geim, S. V. Morozov, D. Jiang, M. I. Katsnelson, I. V. Grigorieva, S. V. Dubonos, and A. A. Firsov, Two-dimensional gas of massless Dirac fermions in graphene, Nature (London) **438**, 197 (2005).

[5] D Xiao, G.-B. Liu, W. Feng, X. Xu, and W. Yao, Coupled Spin and Valley Physics in Monolayers of MoS_2 and Other Group-VI Dichalcogenides, Phys. Rev. Lett. **108**, 196802 (2012).

[6] K. F. Mak, K. L. McGill, J. Park, and P. L. McEuen, The valley Hall effect in MoS_2 transistors, Science **344**, 1489 (2014).

[7] N. Ubrig, S. Jo, M. Philippi, D. Costanzo, H. Berger, A. B. Kuzmenko, and A. F. Morpurgo, Microscopic origin of the valley Hall effect in transition metal dichalcogenides revealed by wavelength-dependent mapping, Nano Lett. **17**, 5719 (2017).

[8] V. M. Kovalev, W.-K. Tse, M. V. Fistul, and I. G. Savenko, Valley Hall transport of photon-dressed quasiparticles in two-dimensional Dirac semiconductors, New J. Phys. **20**, 083007 (2018).

[9] O. V. Kibis, K. Dini, I. V. Iorsh, and I. A. Shelykh, All-optical band engineering of gapped Dirac materials, Phys. Rev. B **95**, 125401 (2017).

[10] J. Tuorila, M. Silveri, M. Sillanpää, E. Thuneberg, Yu. Makhlin, and P. Hakonen, Stark Effect and Generalized Bloch-Siegert Shift in a Strongly Driven Two-Level System, Phys. Rev. Lett. **105**, 257003 (2010).

[11] L. Allen and J. H. Eberly, *Optical Resonance and Two-Level Atoms* (Dover Publications, New York, 1987).

[12] O. Kibis, Dissipationless Electron Transport in Photon-Dressed Nanostructures, Phys. Rev. Lett. **107**, 106802 (2011).

[13] A. D. Wieck, H. Sigg, and K. Ploog, Observation of Resonant Photon Drag in a Two-Dimensional Electron Gas, Phys. Rev. Lett. **64**, 463 (1990).

[14] M. M. Glazov and S. D. Ganichev, High frequency electric field induced nonlinear effects in graphene, Phys. Rep. **535**, 101 (2014).

[15] M. V. Entin, L. I. Magarill, and D. L. Shepelyansky, Theory of resonant photon drag in monolayer graphene, Phys. Rev. B **81**, 165441 (2010).

[16] M. V. Boev, V. M. Kovalev, and I. G. Savenko, Resonant photon drag of dipolar excitons, JETP Lett. **107**, 737 (2018); V. M. Kovalev, M. V. Boev, and I. G. Savenko, Proposal for frequency-selective photodetector based on the resonant photon drag effect in a condensate of indirect excitons, Phys. Rev. B **98**, 041304(R) (2018); V. M. Kovalev, A. E. Miroshnichenko, and I. G. Savenko, Photon drag of a Bose-Einstein condensate, Phys. Rev. B **98**, 165405 (2018).

[17] Zh. Sun, D. N. Basov, and M. M. Fogler, Third-order optical conductivity of an electron fluid, Phys. Rev. B **97**, 075432 (2018).

[18] M. V. Entin, L. I. Magarill, and V. M. Kovalev, Photogalvanic effect in monolayer transition metal dichalcogenides under double illumination, J. Phys. Condens. Matter **31**, 325302 (2019); V. M. Kovalev and I. G. Savenko, Photogalvanic currents in dynamically gapped transition

metal dichalcogenide monolayers, Phys. Rev. B **99**, 075405 (2019).
[19] V. I. Belinicher and B. I. Sturman, The photogalvanic effect in media lacking a center of symmetry, Sov. Phys. Usp. **23**, 199 (1980).
[20] W.-Y. Shan, J. Zhou, and Di Xiao, Optical generation and detection of pure valley current in monolayer transition-metal dichalcogenides, Phys. Rev. B **91**, 035402 (2015).
[21] L. E. Golub, S. A. Tarasenko, M. V. Entin, and L. I. Magarill, Valley separation in graphene by polarized light, Phys. Rev. B **84**, 195408 (2011).
[22] H. Yu, Y. Wu, G.-B. Liu, X. Xu, and W. Yao, Nonlinear Valley and Spin Currents from Fermi Pocket Anisotropy in 2D Crystals, Phys. Rev. Lett. **113**, 156603 (2014).
[23] Y. J. Zhang, T. Oka, R. Suzuki, J. T. Ye, and Y. Iwasa, Electrically switchable chiral light-emitting transistor, Science **344**, 725 (2014).
[24] L. E. Golub and S. A. Tarasenko, Valley polarization induced second harmonic generation in graphene, Phys. Rev. B **90**, 201402(R) (2014).
[25] R. R. Hartmann and M. E. Portnoi, *Optoelectronic Properties of Carbon-Based Nanostructures: Steering Electrons in Graphene by Electromagnetic Fields* (LAP LAMBERT Academic Publishing, Saarbrucken, 2011).
[26] M.-C. Chang and Q. Niu, Berry phase, hyperorbits, and the Hofstadter spectrum: Semiclassical dynamics in magnetic Bloch bands, Phys. Rev. B **53**, 7010 (1996).
[27] M. V. Berry, Quantal phase factors accompanying adiabatic changes, Proc. R. Soc. A **392**, 45 (1984).
[28] N. Nagaosa, J. Sinova, S. Onoda, A. H. MacDonald, and N.-P. Ong, Anomalous Hall effect, Rev. Mod. Phys. **82**, 1539 (2010).
[29] D. J. Thouless, M. Kohmoto, M. P. Nightingale, and M. den Nijs, Quantized Hall Conductance in a Two-Dimensional Periodic Potential, Phys. Rev. Lett. **49**, 405 (1982).
[30] M. Z. Hasan and C. L. Kane, Topological insulators, Rev. Mod. Phys. **82**, 3045 (2010).
[31] Q. Niu and D. J. Thouless, Quantised adiabatic charge transport in the presence of substrate disorder and many-body interaction, J. Phys. A **17**, 2453 (1984).
[32] D. Xiao, Y. Yao, Zh. Fang, and Q. Niu, Berry-Phase Effect in Anomalous Thermoelectric Transport, Phys. Rev. Lett. **97**, 026603 (2006).
[33] D. Xiao, M.-C. Chang, and Q. Niu, Berry phase effects on electronic properties, Rev. Mod. Phys. **82**, 1959 (2010).
[34] Y. Zhang, Y. W. Tan, H. L. Stormer, and P. Kim, Experimental observation of the quantum Hall effect and Berry's phase in graphene, Nature (London) **438**, 201 (2005).
[35] J.-S. You, S. Fang, S.-Y. Xu, E. Kaxiras, and T. Low, Berry curvature dipole current in the transition metal dichalcogenides family, Phys. Rev. B **98**, 121109(R) (2018).
[36] A. Wixforth, J. Scriba, M. Wassermeier, J. P. Kotthaus, G. Weimann, and W. Schlapp, Surface acoustic waves on $GaAs/Al_xGa_{1-x}As$ heterostructures, Phys. Rev. B **40**, 7874 (1989).
[37] R. L. Willet, M. A. Paalanen, R. R. Ruel, K. W. West, L. N. Pfeiffer, and B. J. Bishop, Anomalous Sound Propagation at $\nu = 1/2$ in a 2D Electron Gas: Observation of a Spontaneously Broken Translational Symmetry?, Phys. Rev. Lett. **65**, 112 (1990).
[38] S. H. Zhang and W. Xu, Absorption of surface acoustic waves by graphene, AIP Adv. **1**, 022146 (2011).
[39] V. Miseikis, J. E. Cunningham, K. Saeed, R. O'Rorke, and A. G. Davies, Acoustically induced current flow in graphene, Appl. Phys. Lett. **100**, 133105 (2012).
[40] V. Parente, A. Tagliacozzo, F. von Oppen, and F. Guinea, Electron-phonon interaction on the surface of a three-dimensional topological insulator, Phys. Rev. B **88**, 075432 (2013).
[41] L. L. Li and W. Xu, Absorption of surface acoustic waves by topological insulator thin films, Appl. Phys. Lett. **105**, 063503 (2014).
[42] E. G. Batyev, V. M. Kovalev, and A. V. Chaplik, Response of a Bose-Einstein condensate of dipole excitons to static and dynamic perturbations, JETP Lett. **99**, 540 (2014).
[43] M. V. Boev, A. V. Chaplik, and V. M. Kovalev, Interaction of Rayleigh waves with 2D dipolar exciton gas: Impact of Bose-Einstein condensation, J. Phys. D **50**, 484002 (2017).
[44] V. M. Kovalev and A. V. Chaplik, Effect of exciton dragging by a surface acoustic wave, JETP Lett. **101**, 177 (2015); Acousto-exciton interaction in a gas of 2D indirect dipolar excitons in the presence of disorder, JETP **122**, 499 (2016).
[45] A. Esslingen, A. Wixforth, R. W. Winkler, J. P. Kotthaus, H. Nickel, W. Schlapp, and R. Losch, Acoustoelectric study of localized states in the quantized Hall effect, Solid State Commun. **84**, 939 (1992).
[46] R. H. Parmenter, The acousto-electric effect, Phys. Rev. **89**, 990 (1953).
[47] A. Kormanyos, G. Burkard, M. Gmitra, J. Fabian, V. Zolyomi, N. D. Drummond, and V. Fal'ko, **kp** theory for two-dimensional transition metal dichalcogenide semiconductors, 2D Mater. **2**, 049501 (2015).
[48] M. V. Krasheninnikov and A. V. Chaplik, Plasma-acoustic waves on the surface of a piezoelectric crystal, JETP **48**, 960 (1978).
[49] C. Kittel, *Quantum Theory of Solid States* (Wiley, New York, 2004).
[50] See Supplemental Material at http://link.aps.org/supplemental/10.1103/PhysRevLett.122.256801 for the details of the derivations of the trigonal warping and Hall electric current densities.
[51] V. I. Falko, S. V. Meshkov, and S. V. Iordanskii, Acousto-electric drag effect in the two-dimensional electron gas at strong magnetic field, Phys. Rev. B **47**, 9910 (1993).